



CHORUS

This is the accepted manuscript made available via CHORUS. The article has been published as:

Generalized-gradient-approximation noninteracting free-energy functionals for orbital-free density functional calculations

Valentin V. Karasiev, Travis Sjostrom, and S. B. Trickey
Phys. Rev. B **86**, 115101 — Published 4 September 2012
DOI: [10.1103/PhysRevB.86.115101](https://doi.org/10.1103/PhysRevB.86.115101)

Generalized Gradient Approximation Non-interacting Free Energy Functionals for Orbital-free Density Functional Calculations

Valentin V. Karasiev,^{1,*} Travis Sjoström,¹ and S.B. Trickey¹

¹*Quantum Theory Project, Departments of Physics and of Chemistry,
P.O. Box 118435, University of Florida, Gainesville FL 32611-8435*

(Dated: 07 August 2012)

We develop a framework for orbital-free generalized gradient approximations (GGAs) for the non-interacting free energy density and its components (kinetic energy, entropy) based upon analysis of the corresponding gradient expansion. From that we obtain a new finite-temperature GGA (ftGGA) pair. We discuss implementation of the finite-temperature Thomas-Fermi, second-order gradient expansion, and our new ftGGA free energy functionals in an orbital-free density functional theory (OF-DFT) code, including the construction and validation of required local pseudopotentials. Then we compare results of self-consistent OF-DFT calculations on hydrogen using those non-interacting free energy functionals (in combination with the zero-temperature local density approximation (LDA) for exchange-correlation) with results from conventional finite-temperature Kohn-Sham calculations and the same LDA. As an aid to implementation, we provide analytical expressions for the temperature-dependent scaling factors involved.

PACS numbers:

I. INTRODUCTION

Warm dense matter (WDM) is characterized by elevated temperature (up to one hundred eV) and high pressures (up to hundreds of TPa). These characteristics differ greatly from those in standard condensed matter physics, yet such temperatures and pressures are not high enough to make standard plasma physics methods fully applicable. The typical present-day theoretical and computational approach to WDM thus is a combination of finite-temperature density functional theory to describe the electrons¹⁻³ and classical molecular dynamics for ions. Finite-temperature DFT for the electronic degrees of freedom is realized via the Kohn-Sham (KS) procedure. It becomes computationally very expensive at elevated temperature because of the large number of fractionally occupied KS orbitals which must be taken into account. (The computational cost of solving the KS equations in an atom-centered basis scales in principle as N^4 , where N is proportional to the number of occupied KS orbitals. Obviously N increases with temperature. Variational Coulomb fitting⁴ reduces the scaling to N^3 . In a plane-wave basis with pseudopotentials, the general scaling is N^3 also. Less costly schemes eventually exploit some form of matrix sparsity, thus are not generally applicable.)

In contrast, the orbital-free version of density functional theory (OF-DFT) is, in principle at least, a much less expensive alternative to the orbital-based KS method for both zero-temperature and finite-temperature calculations. OF-DFT scales only with the cell size, so the computational cost of a well-implemented OF-DFT scheme should be about the same for both zero- and finite-temperature regimes.

OF-DFT at zero temperature requires reliable approx-

imations for the exchange-correlation (XC) and non-interacting kinetic energy (KE) T_s density functionals. These two contribute to the total energy E_{tot} with substantially different magnitudes: $T_s \approx |E_{\text{tot}}|$ while $|E_{\text{xc}}|$ is about one order of magnitude smaller. Because of this disparity, development of accurate approximate OF-KE functionals is a challenging task which has not reached the refinement of E_{xc} functionals.

The standard developmental approach to non-empirical E_{xc} approximations invokes a sequence of added functional variables, hence the local density approximation (LDA), gradient expansion approximation (GEA) and generalized gradient approximations (GGA), meta-GGAs (which add the KE density or Laplacian of the density), etc. Functional construction is facilitated by enforcement of known properties of the exact functional. Examples include the highly popular PBE $E_{\text{x,GGA}}$ ⁵ and proposed improvements on it⁶⁻⁸. The GGA approach to the KE functional also is based on satisfaction of some of the known exact conditions on this functional^{9,10}. “Modified conjoint” GGA type KE functionals^{11,12}, for example, are constrained to satisfy one of the important exact conditions, namely, positivity of the functional itself and of the so-called Pauli potential associated with it.

Fortunately, the high density and elevated temperature of the WDM regime is favorable for use of the OF-DFT approach. In finite-temperature OF-DFT, the task is to approximate the entire free energy (non-interacting KE, non-interacting entropy, and XC) as a functional of the electronic density. At present, the basic Thomas-Fermi (TF)^{13,14} model and TF with gradient corrections are the dominant computational approaches in finite-temperature OF-DFT^{15,16}. Renewed interest in better free-energy density functionals is exemplified by two re-

cent studies of their scaling behavior^{17,18}. Here we develop a finite-temperature GGA (ftGGA) approximation for the non-interacting free energy functional. ftGGA is a non-trivial extension of the zero-temperature GGA to finite-temperatures for, as we shall show, it should depend upon explicitly temperature-dependent variables which are defined on the basis of the gradient expansion for the kinetic and entropic contributions to the free energy. Those variables play roles analogous with the reduced density gradient in ground-state functionals.

Pseudopotentials (PPs) are an important implementational challenge in this context. Standard Kohn-Sham calculations on extended, periodically bounded systems most commonly employ PP techniques. In DFT codes of both the plane-wave and numerical grid varieties, PPs reduce computational cost by eliminating the bare Coulomb nuclear-electron singularity and by reducing (substantially) the number of active electrons in the self-consistent field (SCF) procedure. The most common standard PPs are non-local (see for example Refs. 19–21), *i.e.*, there is a different operator for each atomic orbital angular momentum. While the computational cost of OF-DFT does not depend on the total number of electrons, the problems from the singularity of the bare Coulomb external potential remain if one intends to use a plane-wave basis or numerical grid. For OF-DFT in such an implementation, a *local* PP or regularized potential is inescapable.

II. ORBITAL-FREE NON-INTERACTING FREE ENERGY FUNCTIONALS

A. Finite-temperature DFT summary

For development of the finite-temperature version of DFT it is customary to work in the grand canonical ensemble. The grand canonical potential of a system of electrons in an external potential $v(\mathbf{r})$ with electronic density $n(\mathbf{r})$, chemical potential μ , and temperature T can be written as a functional of the density^{1,2}

$$\Omega[n] = \mathcal{F}[n] + \int (v(\mathbf{r}) - \mu)n(\mathbf{r})d\mathbf{r}. \quad (1)$$

The universal free-energy functional $\mathcal{F}[n]$ has the decomposition

$$\mathcal{F}[n] = \mathcal{F}_s[n] + \mathcal{F}_H[n] + \mathcal{F}_{xc}[n], \quad (2)$$

where $\mathcal{F}_s[n]$ is the non-interacting free energy, $\mathcal{F}_H[n]$ is the classical Coulomb repulsion energy, and $\mathcal{F}_{xc}[n]$ is the exchange-correlation contribution to the free energy. In order, these are

$$\mathcal{F}_s[n] = \mathcal{T}_s[n] - T\mathcal{S}_s[n], \quad (3)$$

where \mathcal{T}_s and \mathcal{S}_s are the non-interacting kinetic energy and entropy respectively, and

$$\mathcal{F}_H[n] = \frac{1}{2} \int \int \frac{n(\mathbf{r})n(\mathbf{r}')}{|\mathbf{r} - \mathbf{r}'|} d\mathbf{r}d\mathbf{r}' \quad (4)$$

is the Hartree (classical Coulomb repulsion) energy. The exchange-correlation (XC) functional is

$$\begin{aligned} \mathcal{F}_{xc}[n] &= (\mathcal{T}[n] - \mathcal{T}_s[n]) - T(\mathcal{S}[n] - \mathcal{S}_s[n]) \\ &+ (\mathcal{U}_{ee}[n] - \mathcal{F}_H[n]). \end{aligned} \quad (5)$$

In it, $\mathcal{T}[n]$ and $\mathcal{S}[n]$ are the fully interacting system kinetic energy and entropy respectively and \mathcal{U}_{ee} is the full electron-electron Coulomb interaction energy.

B. Thomas-Fermi approximation

Evaluation of the grand potential Eq. (1) for the *non-interacting* uniform electron gas (UEG) of constant density n in a volume V (with uniform background for charge neutrality; see discussion on this point in Ref. 22) gives the UEG free energy,

$$\begin{aligned} \mathcal{F}_s^{\text{UEG}}(n, T) &= \Omega_s^{\text{UEG}}(n) - \mu \left(\frac{\partial \Omega_s^{\text{UEG}}(n)}{\partial \mu} \right)_{T,V} \\ &= V \frac{\sqrt{2}}{\pi^2 \beta^{5/2}} \left[-\frac{2}{3} I_{3/2}(\beta\mu) + \beta\mu I_{1/2}(\beta\mu) \right]. \end{aligned} \quad (6)$$

Here, $\beta = (k_B T)^{-1}$ and I_α is the Fermi-Dirac integral²³

$$\begin{aligned} I_\alpha(\eta) &:= \int_0^\infty dx \frac{x^\alpha}{1 + \exp(x - \eta)}, \quad \alpha > -1 \\ I_{\alpha-1}(\eta) &= \frac{1}{\alpha} \frac{d}{d\eta} I_\alpha(\eta) \end{aligned} \quad (7)$$

The chemical potential μ is determined from

$$n = -\frac{1}{V} \frac{\partial \Omega}{\partial \mu} \Big|_{T,V} = \frac{\sqrt{2}}{\pi^2 \beta^{3/2}} I_{1/2}(\beta\mu). \quad (8)$$

Invocation of the local density approximation gives the Thomas-Fermi (TF)^{13,14} non-interacting free energy density¹⁵ as

$$\begin{aligned} f_s^{\text{TF}}(n(\mathbf{r}), T) &\equiv \left(\frac{1}{V} \mathcal{F}_s^{\text{UEG}} \right) \Big|_{n=n(\mathbf{r})} \\ &= \frac{\sqrt{2}}{\pi^2 \beta^{5/2}} \left[-\frac{2}{3} I_{3/2}(\beta\mu) + \beta\mu I_{1/2}(\beta\mu) \right]. \end{aligned} \quad (9)$$

Here μ is the local TF chemical potential defined by $n(\mathbf{r})$ through Eq. (8), and not the chemical potential of the non-uniform system. The LDA non-interacting free energy functional is then

$$\mathcal{F}_s^{\text{TF}}[n] = \int f_s^{\text{TF}}(n(\mathbf{r}), T) d\mathbf{r}. \quad (10)$$

The corresponding entropy and kinetic energy densities then follow from Eq. (9):

$$\begin{aligned}\sigma_s^{\text{TF}}(n, T) &= -\left.\frac{\partial f_s^{\text{TF}}(n, T)}{\partial T}\right|_n \\ &= \frac{\sqrt{2}}{\pi^2 \beta^{5/2} T} \left[\frac{5}{3} I_{3/2}(\beta\mu) - \beta\mu I_{1/2}(\beta\mu) \right],\end{aligned}\quad (11)$$

and

$$\begin{aligned}\tau_s^{\text{TF}}(n, T) &= f_s^{\text{TF}}(n, T) + T\sigma_s^{\text{TF}}(n, T) \\ &= \frac{\sqrt{2}}{\pi^2 \beta^{5/2}} I_{3/2}(\beta\mu).\end{aligned}\quad (12)$$

In terms of the reduced temperature

$$t = T/T_F = \frac{2}{\beta[3\pi^2 n(\mathbf{r})]^{2/3}},\quad (13)$$

Eq. (8) gives

$$I_{1/2}(\beta\mu) = \frac{n\pi^2 \beta^{3/2}}{\sqrt{2}} = \frac{2}{3t^{3/2}}.\quad (14)$$

Because $I_{1/2}(x)$ is strictly increasing with x , $(\beta\mu)$ is a function of t , hence all functions of $(\beta\mu)$ are functions of t . As a consequence, the entire term in parenthesis in Eq. (9) also is a function of t . This insight, in combination with the zero-temperature TF kinetic energy density,

$$\tau_0^{\text{TF}}(n) = \frac{3}{10}(3\pi^2)^{2/3} n^{5/3} = \frac{2}{5} \frac{\sqrt{2}}{\pi^2 \beta^{5/2} t^{5/2}},\quad (15)$$

allows Eq. (9) to be presented in the factorized form

$$f_s^{\text{TF}}(n, T) = \tau_0^{\text{TF}}(n)\kappa(t)\quad (16)$$

where

$$\kappa(t) := \frac{5}{2}t^{5/2} \left[-\frac{2}{3}I_{3/2}(\beta\mu) + \beta\mu I_{1/2}(\beta\mu) \right].\quad (17)$$

To facilitate computation, an analytical fit to $\kappa(t)$ is provided in Appendix A.

The correspondingly factorized entropy and kinetic energy densities may be found from Eq. (16) as

$$\begin{aligned}\sigma_s^{\text{TF}}(n, T) &= -\left.\frac{\partial f_s^{\text{TF}}(n, T)}{\partial T}\right|_n \equiv \frac{1}{T}\tau_0^{\text{TF}}(n)\zeta(t), \\ \zeta(t) &= -t\frac{\partial\kappa(t)}{\partial t}\end{aligned}\quad (18)$$

and

$$\begin{aligned}\tau_s^{\text{TF}}(n, T) &= f_s^{\text{TF}}(n, T) + T\sigma_s^{\text{TF}}(n, T) \equiv \tau_0^{\text{TF}}(n)\xi(t) \\ \xi(t) &= \kappa(t) - t\frac{\partial\kappa(t)}{\partial t}.\end{aligned}\quad (19)$$

Fig. 1 shows the functions $\kappa(t)$, $\zeta(t)$, $\xi(t)$, and $\tilde{h}(t)$. (The last-named of these is discussed in the next Section.)

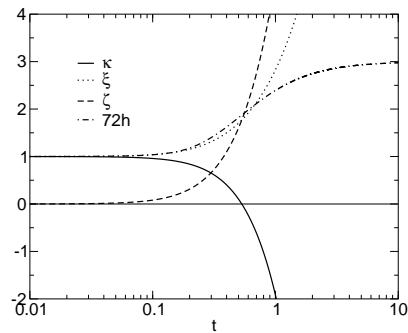


FIG. 1: Behavior of functions κ , ζ , ξ , and $\tilde{h} \equiv 72h$.

The zero-temperature limit for the entropic contribution $T\sigma_s^{\text{TF}}$ and the kinetic energy τ_s^{TF} may be found from Eqs. (11) and (12)

$$\lim_{T \rightarrow 0} T\sigma_s^{\text{TF}}(n, T) = 0,\quad (20)$$

and

$$\lim_{T \rightarrow 0} \tau_s^{\text{TF}} = \tau_0^{\text{TF}}(n).\quad (21)$$

To evaluate these limits, the properties of Fermi-Dirac integrals, $\lim_{\beta \rightarrow \infty} I_{1/2}(\beta\mu) = \frac{2}{3}(\beta\mu)^{3/2}$, $\lim_{\beta \rightarrow \infty} I_{3/2}(\beta\mu) = \frac{2}{5}(\beta\mu)^{5/2}$, and the relation $n = (2\mu)^{3/2}/(3\pi^2)$ obtained from Eq. (8) in the limit $\beta \rightarrow \infty$ were used. From Eqs. (20)-(21) (alternatively, from Eqs. (18)-(19)) and from the non-negativity of the entropy, Eq. (11), and the kinetic energy density, it follows that

$$\begin{aligned}\lim_{T \rightarrow 0} \zeta(t) &= 0, \\ \zeta(t) &\geq 0, \quad \forall t,\end{aligned}\quad (22)$$

and

$$\begin{aligned}\lim_{T \rightarrow 0} \xi(t) &= 1, \\ \xi(t) &\geq 0, \quad \forall t.\end{aligned}\quad (23)$$

C. Gradient expansion

The zero-temperature gradient correction to the Thomas-Fermi model was generalized to finite temperatures by Perrot¹⁶, with higher order corrections given in Ref. 23. In the limit $T \rightarrow 0$, that generalization reduces to the zero-temperature second-order gradient approximation (SGA)²⁴. The finite-temperature gradient term has the form of the von Weizsäcker²⁵ (VW) kinetic energy density, $t_W(n, \nabla n) = |\nabla n|^2/(8n)$, scaled by a function $h(t)$ of the reduced temperature, namely

$$f_s^{\text{SGA}}(n, \nabla n, T) = f_s^{\text{TF}}(n, T) + 8h(t)t_W(n, \nabla n).\quad (24)$$

This follows by elimination of $\beta\mu$ in favor of t (recall Eq. (14)) in Perrot's expression¹⁶

$$h(t) = -\frac{1}{24} \frac{I_{1/2}(\beta\mu)I_{-3/2}(\beta\mu)}{I_{-1/2}^2(\beta\mu)}. \quad (25)$$

It is convenient to use the quantity $\tilde{h}(t) = 72h(t)$, because $\lim_{t \rightarrow 0} \tilde{h}(t) = 1$, which allows us to write the full von Weizsäcker term as $\tilde{h}t_W$ and the corresponding SGA in the more familiar form $(1/9)\tilde{h}t_W$. We adopt the analytical fit of Eq. (25) given in Ref. 16 to a function of reduced temperature t as shown in Appendix A.

For further analysis, it is convenient to introduce the reduced density gradient familiar in zero-temperature GGAs for exchange and KE, namely

$$s(n, \nabla n) \equiv \frac{|\nabla n|}{(2k_F)n} = \frac{1}{2(3\pi^2)^{1/3}} \frac{|\nabla n|}{n^{4/3}}, \quad (26)$$

and rewrite Eq. (24) as

$$f_s^{\text{SGA}}(n, \nabla n, T) = \tau_0^{\text{TF}}(n)\kappa(t) + \tau_0^{\text{TF}}(n)\frac{5}{27}s^2\tilde{h}(t), \quad (27)$$

where the VW term is rewritten as $t_W = \frac{5}{3}\tau_0^{\text{TF}}s^2$.

The kinetic energy and entropy contributions to the free energy functional defined by Eq. (27) may be evaluated as usual (see also Refs. 23,26). First,

$$\begin{aligned} \sigma_s^{\text{SGA}}(n, \nabla n, T) &= -\left. \frac{\partial f_s^{\text{SGA}}(n, \nabla n, T)}{\partial T} \right|_n \\ &= \frac{1}{T}\tau_0^{\text{TF}}(n)\zeta(t) \left(1 - \frac{5}{27}s^2 \frac{t}{\zeta(t)} \frac{d\tilde{h}(t)}{dt} \right). \end{aligned} \quad (28)$$

Then $\tau_s^{\text{SGA}} = f_s^{\text{SGA}} + T\sigma_s^{\text{SGA}}$ gives

$$\begin{aligned} \tau_s^{\text{SGA}}(n, \nabla n, T) &= \tau_0^{\text{TF}}(n)\xi(t) \times \\ &\left(1 + \frac{5}{27}s^2 \frac{1}{\xi(t)} \left[\tilde{h}(t) - t \frac{d\tilde{h}(t)}{dt} \right] \right), \end{aligned} \quad (29)$$

where we have taken into account the definition Eq. (13) and simplified the derivative term in Eqs. (28)-(29) according to $T(\partial\tilde{h}(t)/\partial T)_n = t d\tilde{h}(t)/dt$.

In the zero-temperature limit, the entropic contribution to the free energy of course vanishes, $\lim_{T \rightarrow 0}(T\sigma_s^{\text{SGA}}) = 0$, and the kinetic energy part reduces to the zero-temperature SGA kinetic energy, $\lim_{T \rightarrow 0} \tau_s^{\text{SGA}} = \tau_0^{\text{TF}}(n)(1 + \frac{5}{3}s^2)$.

D. Finite-temperature generalized gradient approximation

The underlying concept of GGAs in zero-temperature XC and KE functionals is to take into account the physical content of higher-order terms in the gradient expansion and effects beyond the slowly varying density

approximation while avoiding difficulties associated with use of a strict second-order expansion as a general functional. For X and KE, this generalization is done by multiplying the relevant LDA (zero-order term) energy density by an enhancement factor which is a functional of the reduced density gradient s , Eq. (26). Both the analytical form and parameters of the enhancement factors may be defined (or at least constrained) by imposition of known exact conditions. We follow an analogous strategy here for the finite-temperature non-interacting system.

The correction terms in Eqs. (27)-(29) are the first terms of a general gradient expansion for the non-interacting free energy and its components (again, see Refs. 23,26). In the finite-temperature case, the structure of Eqs. (28)-(29), suggests that we define corresponding finite-temperature reduced density gradients as

$$\begin{aligned} s_\sigma(n, \nabla n, T) &= s(n, \nabla n) \sqrt{\frac{t d\tilde{h}(t)/dt}{\zeta(t)}}, \\ s_\tau(n, \nabla n, T) &= s(n, \nabla n) \sqrt{\frac{\tilde{h}(t) - t d\tilde{h}(t)/dt}{\xi(t)}}, \end{aligned} \quad (30)$$

for use in the entropy and kinetic energy respectively. It is straightforward to show that in the zero-temperature limit

$$\lim_{T \rightarrow 0} s_\tau(n, \nabla n, T) = s(n, \nabla n). \quad (31)$$

Figure 2 shows the ratios $(s_\tau/s)^2$ and $(s_\sigma/s)^2$ as functions of reduced temperature t . Both are smooth, non-negative functions with some structure at intermediate t . Both vanish at $t \gg 1$. The ratio $(s_\tau/s)^2$ goes to a constant at $t \ll 1$, namely $\lim_{t \rightarrow 0} (s_\tau/s)^2 = 1$. Direct numerical evaluation shows that $(s_\sigma/s)^2 \approx 0.8$ for $t \ll 1$.

With this information, we may define the finite-temperature GGA free energy functional form as

$$\begin{aligned} \mathcal{F}_s^{\text{ftGGA}}[n, T] &= \int \tau_0^{\text{TF}}(n)\xi(t)F_\tau(s_\tau) d\mathbf{r} \\ &- \int \tau_0^{\text{TF}}(n)\zeta(t)F_\sigma(s_\sigma) d\mathbf{r}, \end{aligned} \quad (32)$$

where F_τ and F_σ are the non-interacting kinetic energy and entropic enhancement factors depending on reduced density gradients s_τ and s_σ correspondingly. The definitions in Eq. (32) are generalizations of the second-order gradient expansion of the non-interacting free energy components in Eqs. (28)-(29) in the form of zeroth-order terms multiplied by corresponding enhancement factors. Notice that this definition automatically ensures that the entropic and KE contributions scale correctly, since $T\mathcal{S}_s$ and \mathcal{T}_s scale identically^{17,18}. Specifically, $\mathcal{T}_s^{\text{ftGGA}}[n_\lambda, T] = \lambda^2 \mathcal{T}_s^{\text{ftGGA}}[n, T/\lambda^2]$ and $\mathcal{S}_s^{\text{ftGGA}}[n_\lambda, T] = \mathcal{S}_s^{\text{ftGGA}}[n, T/\lambda^2]$, with $n_\lambda(\mathbf{r}) = \lambda^3 n(\lambda\mathbf{r})$. All of the scaling is in $\tau_0^{\text{TF}}(n)$. All the other factors in

the integrands in Eq. (32) are dimensionless functions of dimensionless variables.

The two RHS terms in Eq. (32) should be interpretable as the kinetic energy ($\mathcal{T}_s^{\text{ftGGA}}$) and entropic ($\text{T}\mathcal{S}_s^{\text{ftGGA}}$) contributions. To enforce this interpretation, we invoke the thermodynamic relation

$$\begin{aligned} \mathcal{S}_s^{\text{ftGGA}} &= -\left. \frac{\partial \mathcal{F}_s^{\text{ftGGA}}}{\partial \text{T}} \right|_{N,V} \\ &= -\left. \frac{\partial \mathcal{T}_s^{\text{ftGGA}}}{\partial \text{T}} \right|_{N,V} + \left. \frac{\partial (\text{T}\mathcal{S}_s^{\text{ftGGA}})}{\partial \text{T}} \right|_{N,V}, \end{aligned} \quad (33)$$

which can be rearranged as

$$\left. \frac{\partial \mathcal{T}_s^{\text{ftGGA}}}{\partial \text{T}} \right|_{N,V} = \text{T} \left. \frac{\partial \mathcal{S}_s^{\text{ftGGA}}}{\partial \text{T}} \right|_{N,V}. \quad (34)$$

Interchange of integration and partial derivative evaluation gives a relation between F_τ and F_σ ,

$$\begin{aligned} \xi'(t)F_\tau(s_\tau) + \xi(t)F'_\tau(s_\tau)\frac{\partial s_\tau}{\partial t} &= \\ -\frac{1}{t}\zeta(t)F_\sigma(s_\sigma) + \zeta'(t)F_\sigma(s_\sigma) + \zeta(t)F'_\sigma(s_\sigma)\frac{\partial s_\sigma}{\partial t}. \end{aligned} \quad (35)$$

Primes denote derivatives with respect to corresponding arguments, *i.e.*, with respect to t , s_τ , or s_σ . Whether or not Eq. (35) is satisfied exactly by a pair of proposed F_τ and F_σ enhancement factors, Eq. (33) always can be used to obtain the entropic contribution, $\text{T}\mathcal{S}_s^{\text{ftGGA}}$, corresponding to a specified ftGGA functional Eq. (32):

$$\begin{aligned} \text{T}\mathcal{S}_s^{\text{ftGGA}}[n, \text{T}] &= -\text{T} \left. \frac{\partial \mathcal{F}_s^{\text{ftGGA}}[n, \text{T}]}{\partial \text{T}} \right|_V \\ &= \int \tau_0^{\text{TF}}(n)t \left[-\xi'(t)F_\tau(s_\tau) - \xi(t)F'_\tau(s_\tau)\frac{\partial s_\tau}{\partial t} \right. \\ &\quad \left. + \zeta'(t)F_\sigma(s_\sigma) + \zeta(t)F'_\sigma(s_\sigma)\frac{\partial s_\sigma}{\partial t} \right] d\mathbf{r}. \end{aligned} \quad (36)$$

There is motivation to satisfy Eq. (35) since the scaling factors ξ and ζ already constrain the terms of Eq. (32) be the kinetic and entropic pieces, respectively, in both the zero-temperature and Thomas-Fermi limits.

However, use of Eq. (35) to determine one of the enhancement factors when the other is given is not straightforward in general. The SGA functionals Eqs. (28) - (29), which do satisfy Eq. (35), provide a clue to a simpler approximate route. Those functionals can be written in the form of Eq. (32) with enhancement factors

$$\begin{aligned} F_\tau^{\text{SGA}}(s_\tau) &= \left(1 + \frac{5}{27}s_\tau^2\right) \\ F_\sigma^{\text{SGA}}(s_\sigma) &= \left(1 - \frac{5}{27}s_\sigma^2\right), \end{aligned} \quad (37)$$

Thus, the two SGA enhancement factors are related by

$$F_\sigma^{\text{SGA}}(s_\sigma) = 2 - F_\tau^{\text{SGA}}(s_\sigma). \quad (38)$$

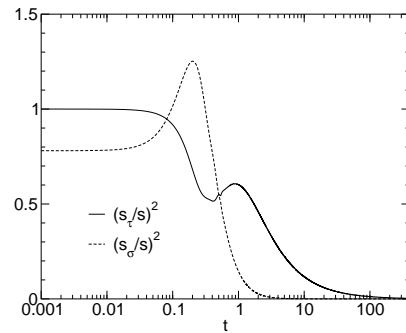


FIG. 2: Functions $(s_\tau/s)^2$ and $(s_\sigma/s)^2$.

Eq. (38) can be generalized in the usual spirit of GGAs by requiring that the entropic contribution enhancement factor associated with a chosen $F_\tau(s_\tau)$, Eq. (32), is

$$F_\sigma(s_\sigma) \approx 2 - F_\tau(s_\sigma), \quad (39)$$

In general, a pair of enhancement factors related in this way will not satisfy Eq. (35) precisely. The main consequence of such a failure is that the two terms in Eq. (32) may not be interpretable strictly as kinetic and entropic contributions. Instead, Eq. (36) gives the entropic contribution, Eq. (32) gives the non-interacting free-energy, and the kinetic energy functional is $\mathcal{T}_s[n, \text{T}] = \mathcal{F}_s[n, \text{T}] + \text{T}\mathcal{S}_s[n, \text{T}]$. A complementary discussion to this approach is given in Appendix B.

The requirement that the zero-temperature limit of the functional $\mathcal{F}_s^{\text{ftGGA}}[n, \text{T}]$, Eq. (32), should reduce to the zero-temperature GGA kinetic energy, in conjunction with the factorized form of the integrand, leads to the realization that the simplest approximation for a finite-temperature GGA F_τ is to use a zero-temperature GGA kinetic energy enhancement factor F_t form in Eq. (32), *i.e.*,

$$F_\tau(s_\tau) \approx F_t(s_\tau). \quad (40)$$

By this argument, the finite-temperature analog of the modified conjoint GGA for the kinetic energy introduced in Refs. 11,12 is the two-parameter KST2 free energy functional $\mathcal{F}_s^{\text{KST2}}[n, \text{T}]$ defined by Eq. (32) with the following enhancement factors

$$\begin{aligned} F_\tau^{\text{KST2}}(s_\tau) &= 1 + \frac{C_1 s_\tau^2}{1 + a_1 s_\tau^2} \\ F_\sigma^{\text{KST2}}(s_\sigma) &= 1 - \frac{C_1 s_\sigma^2}{1 + a_1 s_\sigma^2}, \end{aligned} \quad (41)$$

with $C_1 = 2.03087$, $a_1 = 0.29424$. These are the zero-temperature parameters from Refs. 11,12.

The second enhancement factor, which is nominally entropic, may take negative values, just as for the SGA enhancement factor. However, the relevant positivity constraint is on the entropy, not the entropy density. The

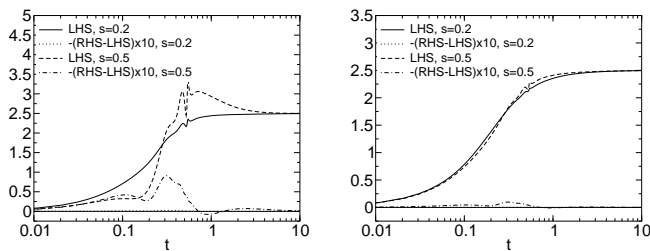


FIG. 3: Left: LHS and RHS-LHS of Eq. (35) evaluated for KST2 enhancement factors, Eq. (41), at $s = 0.2$ and 0.5 . Right: same as left panel, but evaluated for enhancement factors Eq. (41) with parameters defined by the Tran-Wesolowski (TW) kinetic energy functional²⁷.

distinction and challenge for functional design resembles closely the debate over local versus global satisfaction of the Lieb-Oxford bound in exchange functionals; see Ref. 6 and references therein. While we generally favor the argument that universality of a functional compels local enforcement of such constraints *i.e.*, on the free energy densities, here we have chosen to explore the simple form Eq. (41) and confirm *a posteriori* that the total entropy is positive. Numerical results are in Sec. IV.

To test the effects of non-satisfaction of Eq. (35), we have evaluated both sides of that equation with the KST2 functionals and parametrization, Eq. (41). The left-hand panel of Fig. 3 shows the values from the left-hand side (LHS) and the difference between the right-hand side (RHS) and LHS values (RHS-LHS) of Eq. (35) at both $s = 0.2$ and $s = 0.5$. The right-hand panel of that figure shows the same quantities evaluated for enhancement factors of the same form as Eq. (41) but with parameters defined by the zero-temperature orbital-free kinetic energy functional of Tran and Wesolowski (TW)²⁷ (see Section IV for parameter values). The difference (RHS-LHS) is small for both functionals. Although that difference increases with increasing s , one may expect that the second term in Eq. (32) will be close to the proper entropic contribution Eq. (36) for this pair of functionals. Note moreover, that despite the seemingly smaller error of the TW parameterization, in fact KST2 does better in actual calculations; again see Section IV. Eventually the quality of an approximate functional is defined by the quality of its prediction of the non-interacting free energy, \mathcal{F}_s .

We remark that, in all cases, the LHS and the RHS of Eq. (35) are not continuous functions of t at $t \approx t_0$ (see Appendix A), the point at which the two fits for $t \geq t_0$ and $t \leq t_0$ are joined. Clearly at least the second derivative of the fits presented in Appendix A has abrupt behavior at t_0 . Apparently this technical issue traces to Perrot's original fits¹⁶. So far it has not proved problematic but may need to be addressed in the future.

Ref. 28 showed that the simple combination of the

VW and Thomas-Fermi functionals provides total energies and lattice parameters which are reasonably close (at least for a few systems) to those obtained with the mcGGA kinetic energy functional, though the latter functional is better justified formally. Put into ftGGA form, the VWTF kinetic energy has the enhancement factors

$$F_\tau^{\text{VWTF}}(s_\tau) = 1 + \frac{5}{3}s_\tau^2$$

$$F_\sigma^{\text{VWTF}}(s_\sigma) = 1 - \frac{5}{3}s_\sigma^2. \quad (42)$$

Thus we have the corresponding free energy functional $\mathcal{F}_s^{\text{VWTF}}[n, T]$ defined by Eqs. (32) and (42). At $T = 0$ K, this is simply a rearrangement which exposes the TF contribution as the choice of approximation for the so-called Pauli term¹², while at $T > 0$, the T -dependent Thomas-Fermi contribution becomes the finite- T version.

III. IMPLEMENTATION

In Sec. I we remarked that OF-DFT in a plane-wave basis (or on a numerical grid) requires a *local* pseudopotential (LPP) (sometimes known as a regularized potential, depending on the analysis used for development). Since it is desirable to exploit the OF-DFT optimization tools in our modified version of the ground-state PROFESS code^{29,30}, the issue is germane here.

Perhaps the simplest form of regularization is the model potential proposed by Heine and Abarenkov^{31,32}. In real space, it is

$$v_{\text{mod}}(r) = \begin{cases} -A, & r < r_c \\ -Z/r, & r \geq r_c \end{cases} \quad (43)$$

where A is a constant, r_c is the core radius, and Z is the core charge. For use in a plane-wave code, it is convenient to have a reciprocal space representation,

$$v_{\text{mod}}(q) = \frac{-4\pi}{Vq^2} [(Z - Ar_c)\cos(qr_c) + (A/q)\sin(qr_c)]f(q), \quad (44)$$

where V is the unit cell volume. The factor $f(q) = \exp[(-q/q_c)^6]$ is a rounded step-function introduced to suppress spurious oscillations in $v_{\text{mod}}(q)$ caused by the Fourier transform of the discontinuity of the real-space potential at the core radius. This smoothing also ensures rapid decay of $v_{\text{mod}}(q)$ at large wave-vectors (see Ref. 31). In the work reported below, we chose q_c as suggested in that reference, namely, to equal the position of the second zero of $v_{\text{mod}}(q)$.

For this initial study, we focus on Hydrogen. For the H atom we chose $r_c = 0.25$ Bohr in Eq. (43), with the parameter A determined by constraining a KS calculation

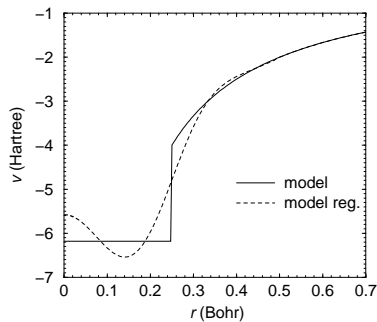


FIG. 4: Model pseudopotential for hydrogen in real space as defined by Eq. (43) and the smoothed version which results from inverse Fourier-Bessel transform of $v_{\text{mod}}(q)$, Eq. (44).

with the local pseudopotential (LPP) Eq. (43) to reproduce the reference optimized simple-cubic Hydrogen (sc-H) lattice constant $a = 1.447 \text{ \AA}$ (see Table I). Those KS calculations were done with Perdew-Zunger (PZ) LDA exchange-correlation³³ in the ABINIT code³⁴. KS reference calculations were performed with the non-local projector augmented wave (PAW) scheme as implemented in ABINIT using cutoff radius $r_c = 0.45$ Bohr. Both the ABINIT PAW and local (model) pseudopotential calculations used an 8-atom unit cell and a $13 \times 13 \times 13$ \mathbf{k} -mesh. For further reference, corresponding bare potential calculations were done with QUANTUM-ESPRESSO³⁵ using a 500 Ry energy cutoff and exactly the same unit cell and \mathbf{k} -mesh.

The optimized parameter values which result are $A = 6.18$ Hartree, $q_c = 29.97 \text{ Bohr}^{-1}$. Figure 4 shows both the original real-space and the back-transformed potential (after reciprocal-space smoothing) for Hydrogen.

Fig. 5 gives a comparison of pressures calculated from the model potential (again with ABINIT) and the bare Coulomb potential (with QUANTUM-ESPRESSO) for standard KS calculations on sc-H at two temperatures; 100K and 100,000K, again with simple PZ LDA. Since we are interested only in the effects of regularization, the deficiencies of ground state LDA-XC as an implicitly temperature-dependent functional are irrelevant. For both electronic temperatures, the pressure from the local (regularized) pseudopotential calculations is in excellent agreement with results from the bare Coulomb nuclear-electron potential calculations. The total-free energies from these two calculations also are in near-perfect agreement: the relative difference between the model potential and the bare Coulomb results does not exceed 0.5% except for a small range of material densities around $\rho_H \approx 6 \text{ g/cm}^3$ for both temperatures, where the absolute value of the total free-energy is close to zero as it crosses from positive to negative values. The upper part of Table I gives a detailed comparison of the equilibrium KS predictions from these various potentials.

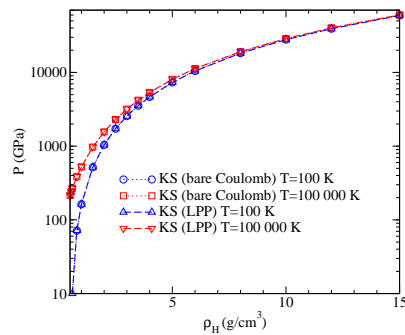


FIG. 5: Test of model potential Eq. (44) for sc-H by comparison between Kohn-Sham results obtained with the bare Coulomb nuclear-electron interaction and those obtained with Eq. (44) (both with PZ LDA XC functional) for $T = 100\text{K}$ and $100,000 \text{ K}$.

TABLE I: Upper panel: Kohn-Sham equilibrium lattice constant a (\AA) and bulk modulus B (GPa) for sc-H calculated with QUANTUM-ESPRESSO plane-wave code (PW) and bare Coulomb potential and with ABINIT PW projector augmented wave (PAW) and model potentials (real and reciprocal space). Lower panel: Comparison of OF-DFT calculations using ftGGA(KST2), ftGGA(TW), ft(VWTF), and ftSGA non-interacting free-energy functionals in combination with zero-temperature PZ LDA exchange-correlation³³ with local pseudopotentials v_{mod} (see text). All calculations are done at electronic temperature $T = 100 \text{ K}$ (ionic temperature $T_{\text{ion}} = 0 \text{ K}$). See text regarding blank entries.

Method	PP	a	B
Kohn-Sham			
PW (QE)	bare Coul.	1.446	108.4
PW (ABINIT)	PAW	1.447	108.3
Kohn-Sham			
PW (ABINIT)	model ^a	1.447	108.1
PW (ABINIT)	model reg. ^b	1.446	108.3
OFDFT			
ftGGA(KST2)	model ^c	1.392	146
ft(VWTF)	model ^c	1.394	146
ftGGA(TW)	model ^c	–	–
ftSGA	model ^c	–	–
ftTF	model ^c	–	–

^aReal space potential defined by Eq. (43).

^bReal space potential defined by inverse Fourier-Bessel transform of Eq. (44).

^cReciprocal space potential defined by Eq. (44).

IV. OF-DFT RESULTS

All our OF-DFT calculations were done with a locally modified version of the PROFESS code^{29,30}. For simplicity and to provide a uniform, clear-cut comparison, all the non-interacting free energy functionals we studied were used in conjunction with the ground state PZ LDA

exchange-correlation functional³³.

We implemented the new ftGGA functionals, Eq. (32), with the enhancement factors defined in Eq. (41) F_τ^{KST2} , F_σ^{KST2} (ftGGA(KST2)). For comparison we also implemented the ft(VWTF) functional, F_τ^{VWTF} , F_σ^{VWTF} , from Eq. (42), and the ftGGA version of the zero-temperature GGA kinetic energy functional parameterized by Tran and Wesolowski (TW)²⁷. The ftGGA(TW) enhancement factors have the form of Eq. (41) but with $C_1 = 0.2319$ and $a_1 = 0.2748$. (In fairness to those authors, the TW parameters were not intended for this purpose.) For reference, we also implemented the familiar finite-temperature TF and ftSGA free energy functionals in the form of Eq. (32), where $F_\tau = F_\sigma = 1$ for ftTF and F_τ, F_σ are defined through Eq. (37) for ftSGA. To our knowledge, the only non-interacting free-energy functionals proposed previously are these last two, ftTF and ftSGA.

Figure 6 compares Kohn-Sham and OF-DFT results for total free energies per atom as a function of material density for sc-H at electronic temperature $T=100$ K. Both calculations were done with the same regularized local potential, Eq. (44). The PROFESS OF-DFT calculation used a 64-atom supercell. The KS calculations with local pseudopotential used an 8-atom cell and a $13 \times 13 \times 13$ \mathbf{k} -mesh. Two functionals, ft(VWTF) and ftGGA(KST2), demonstrate reasonable agreement with the KS reference data. As is evident from that figure, the widely used ftSGA and ftTF functionals, as well as the ftTW functional, do not predict energy minima, at least in the range of densities treated. The lower part of Table I shows OF-DFT results for the equilibrium lattice constant and bulk moduli obtained by fitting the calculated total energies per cell to the stabilized jellium model equation of state (SJEOS)³⁶. Two functionals, ftGGA(KST2) and ft(VWTF), predict quite similar results: the lattice constant is underestimated by three percent, but the bulk modulus is overestimated by about 40%. These results are encouraging as compared to the other three orbital-free functionals.

The left-hand panels of Figures 7-8 compare Kohn-Sham and OF-DFT total free energies per atom as a function of electronic temperature for two material densities, $\rho_H = 2.0$ and 4.0 g/cm^3 . The right-hand panels show relative differences of the OF-DFT values with respect to the Kohn-Sham reference results. At lower temperatures two functionals, ft(VWTF) and ftGGA(KST2), overestimate the total free energy by about 10% and 15% for $\rho_H = 2.0$ and 4.0 g/cm^3 respectively. Two functionals, ftSGA and ftGGA(TW), underestimate the free energy with relative error between 20% and 30% for those two densities. The error of the ftTF functional is much higher, 40% and 65% respectively. It is interesting that the relative error of all functionals remains nearly constant up to $T=100,000$ K, after which that error decreases

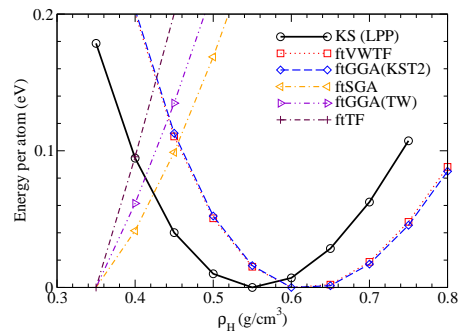


FIG. 6: Total free energy per atom as a function of material density for sc-H at electronic temperature $T=100$ K (ionic temperature $T_{ion} = 0$ K) for LPP KS and OF-DFT calculations (both with PZ LDA XC functional). The LPP is Eq. (44).

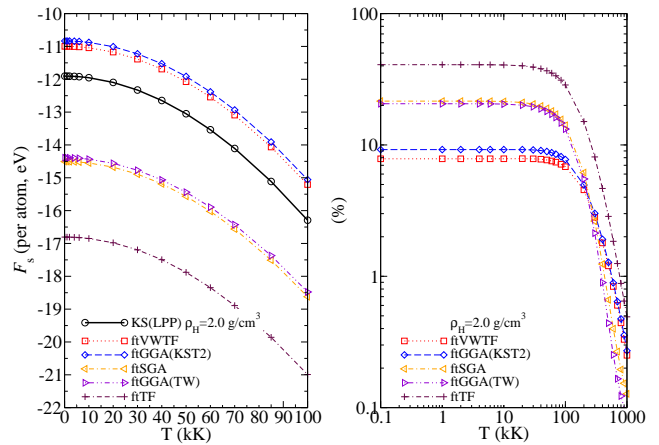


FIG. 7: Left: total free-energy per atom as a function of electronic temperature for LPP KS and OF-DFT calculations (both with PZ LDA XC functional). Right: relative free energy differences with respect to KS values, $|(\mathcal{F}_s - \mathcal{F}_s^{\text{KS}})/\mathcal{F}_s^{\text{KS}}| \times 100\%$ for the ft(VWTF), ftGGA(KST2), ftSGA, ftGGA(TW), and ftTF free energy functionals. Material density $\rho_H = 2.0$ g/cm^3 . The LPP is Eq. (44).

with increasing T . At $T=1,000,000$ K, the relative error of the ftTF functional is about 0.4% and 1% for the two densities respectively, *i.e.*, the high-temperature Thomas-Fermi limit is reached at this point. Also we note that for $T > 200,000$ K ($\rho_H = 2.0$ g/cm^3) and $T > 400,000$ K ($\rho_H = 4.0$ g/cm^3), the relative errors of the ftSGA and ftGGA(TW) functionals become smaller than the errors of the ft(VWTF) and ftGGA(KST2). This behavior may be understood by the fact that for those temperatures the system may be considered as a weakly inhomogeneous gas before reaching the high- T Thomas-Fermi limit. In such circumstances, the second-order gradient approximation should be appropriate.

Figures 9 - 11 compare KS and OF-DFT results for pressure versus material density in sc-H at electronic temperatures $T=100$ K, $50,000$ K, and $100,000$

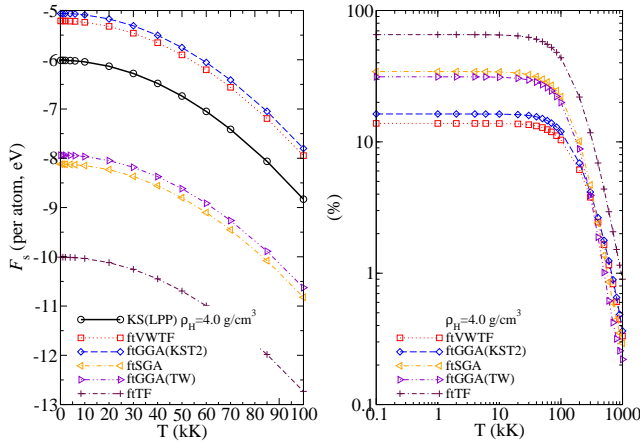


FIG. 8: As in Fig. 7 for $\rho_H = 4.0 \text{ g/cm}^3$.

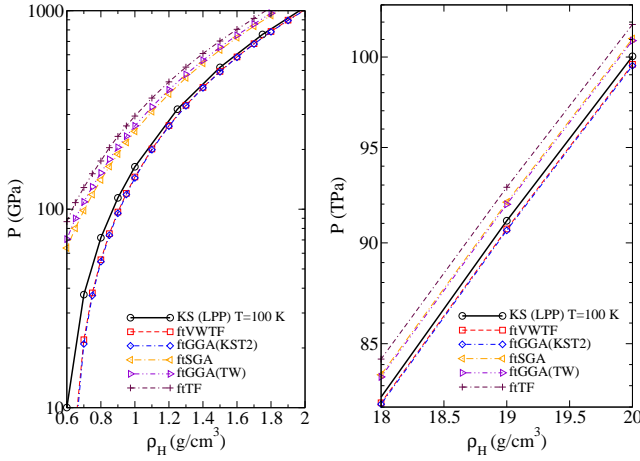


FIG. 9: Pressure as a function of material density (low to intermediate at left, high at right) for sc-H at electronic temperature $T=100 \text{ K}$ for LPP KS and OF-DFT calculations (both with PZ LDA xc functional). The LPP is Eq. (44).

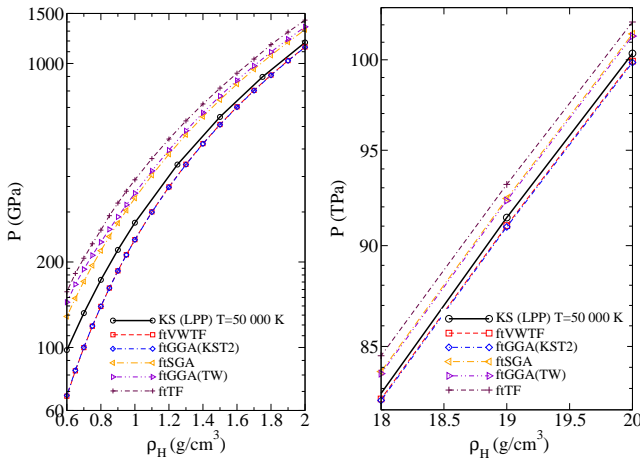


FIG. 10: As in Fig. 9 for electronic temperature $T=50,000 \text{ K}$.

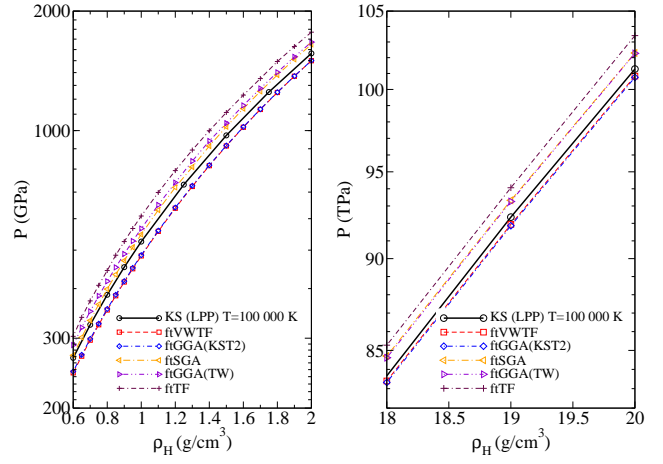


FIG. 11: As in Fig. 9 for electronic temperature $T=100,000 \text{ K}$.

K respectively. At low temperature, the functionals clearly fall into two groups at the lower densities. The ftGGA(KST2) and ft(VWTF) functionals give slightly low pressures compared to the KS result, while the pure ftTF, ftSGA, and ftGGA(TW) functionals yield distinctly higher pressures. For the higher densities, the pressures from all the functionals become closer (as they should, since ftTF is the eventual limit). Similarly, the pressures from all the functionals are closer at $T=50,000 \text{ K}$ and $100,000 \text{ K}$, but two functionals from the first group (ftGGA(KST2) and ft(VWTF)) yield visibly smaller errors compared to the second group for all density ranges and for all electronic temperatures, with one exception, ftSGA. It separates itself from the former second group at $T=100,000 \text{ K}$ and gets closer to the KS behavior in a small range of densities (approximately $0.6 - 1.2 \text{ g/cm}^3$) than at lower temperatures. At $T=50,000 \text{ K}$ and for low densities, the relative error of the first group of functionals (ftSGA, ftGGA(TW) and ftTF) is between 30% and 50%, while the relative error from the ftGGA(KST2) and ft(VWTF) functionals is about 30%. With increasing temperature, for low densities all the functionals give pressures closer to the KS results. At $T=100,000 \text{ K}$, the errors for ftGGA(KST2) and ftSGA are about 7%. At high density for all temperatures, the relative error of the ftGGA(KST2) functional is less than 1%, while the error of functionals from the first group is between 1% and 2%.

Finally, we return to the issue of positivity of the entropy for the KST2 functional. Eq. (35) may be rearranged to the form

$$\begin{aligned}
 T\Delta S_s := & \int \left[-\xi'(t)F_\tau(s_\tau) - \xi(t)F'_\tau(s_\tau) \right] \frac{\partial s_\tau}{\partial t} \\
 & + \zeta'(t)F_\sigma(s_\sigma) + \zeta(t)F'_\sigma(s_\sigma) \frac{\partial s_\sigma}{\partial t} \\
 & - \frac{1}{t} \zeta(t)F_\sigma(s_\sigma) \Big] t\tau_0^{\text{TF}}(n) d\mathbf{r}^3. \quad (45)
 \end{aligned}$$

TABLE II: Non-interacting entropic component of the free-energy functional, TS_s , negative contribution, TS_s^- , and the difference between Eq. (36) and the second term of Eq. (32) for the ftGGA functionals for 1-atom sc-H at density $\rho_H = 0.15 \text{ g/cm}^3$ and ionic temperature $T_{ion} = 0K$. All in eV.

T(K)	ft(VWTF)		ftGGA(KST2)			ftSGA		ftGGA(TW)		
	TS_s	TS_s^-	TS_s	TS_s^-	$\text{T}\Delta\mathcal{S}_s$	TS_s	TS_s^-	TS_s	TS_s^-	$\text{T}\Delta\mathcal{S}_s$
5 000	0.10	0.0	0.10	0.0	0.0	0.10	0.0	0.10	-0.01	-0.01
10 000	0.40	0.0	0.38	0.0	-0.01	0.37	0.0	0.38	-0.02	-0.03
20 000	1.47	0.0	1.48	-0.01	-0.02	1.37	0.0	1.41	-0.07	-0.09
30 000	3.30	0.0	3.32	-0.01	-0.03	2.91	0.0	3.00	-0.12	-0.15
40 000	5.78	0.0	5.85	0.0	-0.02	4.88	0.0	4.98	-0.17	-0.21
50 000	8.69	0.0	8.78	0.0	-0.01	7.23	0.0	7.35	-0.19	-0.25
100 000	26.36	0.0	26.42	0.0	0.0	23.00	0.0	23.1	-0.3	-0.4
250 000	95.11	0.0	95.14	0.0	0.0	93.05	0.0	91.1	-0.3	-0.5
300 000	121.15	0.0	121.18	0.0	0.0	119.69	0.0	117.4	0.0	-0.4
400 000	176.33	0.0	176.36	0.0	0.0	175.40	0.0	174.7	0.0	-0.1
1 000 000	559.03	0.0	559.05	0.0	0.0	558.77	0.0	558.8	0.0	-0.0

By comparison with Eqs. (36) and (32), we recognize immediately that Eq. (45) gives the difference between the GGA entropy defined in Eq. (36) and the entropic contribution from the approximate functional given by the second term in Eq. (32). If Eq. (35) is satisfied exactly, then the bracket in Eq. (45) is zero, hence $\text{T}\Delta\mathcal{S}_s = 0$. Thus we have two ways of assessing the proper behavior of a proposed entropy functional. Table II shows that, at least for the sc-H system, the KST2 GGA enhancement factor defined by Eqs. (41) gives a properly positive entropy. There is little or no contamination by negative contributions relative to the total TS_s value. For material densities at least as low as 0.5 g/cm^3 and higher, the negative contribution to the entropy is zero. Moreover, the deviation from satisfaction of Eq. (35) is small compared to the entropy, that is, $|\text{T}\Delta\mathcal{S}_s|/\text{TS}_s \approx 0$. This is not true for a ftGGA based on a different zero-temperature ofKE functional, as illustrated by the results for ftGGA(TW) in that table. Nevertheless, the behavior of $\text{T}\Delta\mathcal{S}_s$ with increasing temperature is similar for both functionals. Also, the SGA entropy is positive, not an entirely expected result in view of the fact that the SGA enhancement factor $F_\sigma^{\text{SGA}}(s_\sigma)$ can go negative, recall Eq. (37).

V. SUMMARY AND CONCLUSIONS

We have presented a new analytical route for the development of finite-temperature analogs of the GGA for the non-interacting free-energy functional, as well as a simplified version of it. Analysis of the finite-temperature second-order gradient expansion of the free energy leads to the definition of temperature-dependent reduced density gradients for both the kinetic and entropic contributions to the free energy. The dependence of these variables upon reduced temperature t is smooth and they

have proper $t \ll 1$ and $t \gg 1$ behavior. We comment that, in principle one may try to use the gradient expansion for the total non-interacting free energy Eq. (27) to define a corresponding temperature-dependent reduced density gradient s_f , then introduce a ftGGA with a single enhancement factor $F_f(s_f)$. But it becomes clear almost immediately that the variable s_f^2 is not positive definite. Moreover, it has a pole because the function $\kappa(t)$, which appears in the denominator of the variable s_f , has a zero (see Fig. 1). This analysis leads to the conclusion that a finite-T GGA should be constructed with the kinetic and entropic contributions treated separately (as we have done), not combined in a functional with a single enhancement factor.

Such a two-part ftGGA functional is defined completely by a pair of enhancement factors, F_τ and F_σ . From standard thermodynamics, it follows that these enhancement factors are not independent. We have given the formal relationship in Eq. (35) but solution of that equation relating F_τ and F_σ is formidable. As an initial step therefore, we have proposed a simpler approximate relationship between the two enhancement factors and showed that it provides reasonably satisfactory results. In the $T \rightarrow 0$ limit, all ftGGA free energy functionals should reduce to known zero-temperature kinetic energy functionals, a fact we have used to present a new, rather simple ftGGA.

Numerical implementation of the OF-DFT calculations in a plane-wave basis requires a local pseudopotential which we have presented. Comparison of finite temperature OF-DFT and KS calculations on sc-H over a wide range of material densities for electronic temperatures up to 100,000K leads to the conclusions that two ftGGA functionals, namely KST2 and VWTF, provide overall best results and that the relative error in the high density regime is small for all functionals.

Acknowledgments

We acknowledge informative conversations with Frank Harris and Jim Dufty with thanks. This work was supported in substantial part by the U.S. Dept. of Energy TMS grant DE-SC0002139.

Appendix A

The temperature scaling function κ introduced in Eq. (16) may be written by use of Eqs. (9) and (15) as

$$\kappa(\beta\mu) = \frac{5}{2} \left(\frac{3}{2} I_{1/2}(\beta\mu) \right)^{-5/3} \times \left[-\frac{2}{3} I_{3/2}(\beta\mu) + \beta\mu I_{1/2}(\beta\mu) \right]. \quad (\text{A1})$$

For $t \geq t_0 = 0.543010717965$

$$\begin{aligned} \kappa(t) = & -2.5t \ln(t) - 2.141088549t + 0.2210798602t^{-0.5} + 0.7916274395 \times 10^{-3}t^{-2} \\ & - 0.4351943569 \times 10^{-2}t^{-3.5} + 0.4188256879 \times 10^{-2}t^{-5} - 0.2144912720 \times 10^{-2}t^{-6.5} \\ & + 0.5590314373 \times 10^{-3}t^{-8} - 0.5824689694 \times 10^{-4}t^{-9.5} \end{aligned} \quad (\text{A2})$$

$$\begin{aligned} \tilde{h}(t) = & 3 - 0.7996705242t^{-1.5} + 0.2604164189t^{-3} - 0.1108908431t^{-4.5} + 0.6875811936 \times 10^{-1}t^{-6} \\ & - 0.3515486636 \times 10^{-1}t^{-7.5} + 0.1002514804 \times 10^{-1}t^{-9} - 0.1153263119 \times 10^{-2}t^{-10.5} \end{aligned} \quad (\text{A3})$$

For $t \leq t_0 = 0.543010717965$

$$\begin{aligned} \kappa(t) = & 1 - 4.112335167t^2 + 1.995732255t^4 + 14.83844536t^6 - 178.4789624t^8 \\ & + 992.5850212t^{10} - 3126.965212t^{12} + 5296.225924t^{14} - 3742.224547t^{16} \end{aligned} \quad (\text{A4})$$

$$\begin{aligned} \tilde{h}(t) = & 1 + 3.210141829t^2 + 58.30028308t^4 - 887.5691412t^6 + 6055.757436t^8 \\ & - 22429.59828t^{10} + 43277.02562t^{12} - 34029.06962t^{14} \end{aligned} \quad (\text{A5})$$

Appendix B

We outline a route to simplified GGAs which is a potential alternative to the one given in the discussion of Equations (37) - (39). Equations (37) obviously combine to give

$$F_\sigma^{\text{SGA}}(s_\sigma) = 2 + \frac{5}{27}(s_\tau^2 - s_\sigma^2) - F_\tau^{\text{SGA}}(s_\tau) \quad (\text{B1})$$

As suggested in the discussion in conjunction with Fig. 2, the ratio

$$\nu(t) := (s_\sigma(t)/s_\tau(t))^2 \quad (\text{B2})$$

is a smooth, bounded ($0 \leq \nu(t) \lesssim 2.2$) function. See Fig. 12. With this function, Eq. (B1) becomes

$$F_\sigma^{\text{SGA}}(s_\sigma) = 2 + \frac{5}{27}s_\tau^2(1 - \nu(t)) - F_\tau^{\text{SGA}}(s_\tau) \quad (\text{B3})$$

By use of Eq. (14), we may eliminate $(\beta\mu)$ in favor of t in Eq. (A1). We have done that numerically. With that result, we can present $\kappa(t)$ analytically as an adapted form of Perrot's free energy fit¹⁶. See below. The functions $\zeta(t)$ and $\xi(t)$ may be calculated using relations with $\kappa(t)$ given in Eqs. (18)-(19). In addition, we provide an adapted analytical $\tilde{h}(t)$. Both functions are split into regions $t \leq t_0$ and $t \geq t_0$, where $t_0 = 4(2/3\pi^2)^{1/3}/3$, to take account of the different asymptotic forms of the Fermi integrals for $(\beta\mu) \ll 0$ and $(\beta\mu) \gg 0$.

Utilization to form a GGA is via

$$F_\sigma^{\text{GGA}}(s_\sigma) = 2 + \frac{5}{27}s_\tau^2(1 - \nu^{\text{GGA}}(t)) - F_\tau^{\text{GGA}}(s_\tau) \quad (\text{B4})$$

where the superscript ‘‘GGA’’ on ν indicates use of some judiciously selected approximate representation of $\nu(t)$. This choice can be constrained by insertion of the form from Eq. (B4) in Eq. (35). We have this approach under study.

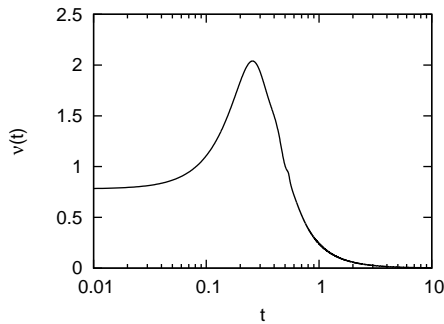


FIG. 12: $\nu(t)$ as defined by Eq. (B2).

-
- * Electronic address: vkarasev@qtp.ufl.edu
- ¹ N.D. Mermin, Phys. Rev. **137**, A1441 (1965).
 - ² M.V. Stoitsov and I.Zh. Petkov, Annals Phys. **185**, 121 (1988).
 - ³ R.M. Dreizler in *The Nuclear Equation of State, Part A*, W. Greiner and H. Stöcker eds., NATO ASI **B216** (Plenum, NY, 1989) 521.
 - ⁴ B.I. Dunlap, N. Rösch, and S.B. Trickey, Mol. Phys. **108**, 3167 (2010).
 - ⁵ J.P. Perdew, K. Burke, and M. Ernzerhof, Phys. Rev. Lett. **77**, 3865 (1996); erratum Phys. Rev. Lett. **78**, 1396 (1997).
 - ⁶ A. Vela, V. Medel, and S.B. Trickey, J. Chem. Phys. **130**, 244103 (2009).
 - ⁷ L.A. Constantin, E. Fabiano, S. Laricchia, and F. Della Sala, Phys. Rev. Lett. **106**, 186406 (2011).
 - ⁸ J.M. del Campo, J.L. Gázquez, S.B. Trickey, and A. Vela, J. Chem. Phys. **136**, 104108 (2012).
 - ⁹ J.P. Perdew, Phys. Lett. A **165**, 79 (1992).
 - ¹⁰ E.V. Ludeña and V.V. Karasiev, in *Reviews of Modern Quantum Chemistry: a Celebration of the Contributions of Robert Parr*, edited by K.D. Sen (World Scientific, Singapore, 2002) p. 612.
 - ¹¹ V.V. Karasiev, S.B. Trickey, and F.E. Harris, J. Comput.-Aided Mat. Des. **13**, 111 (2006).
 - ¹² V.V. Karasiev, R.S. Jones, S.B. Trickey, and F.E. Harris, Phys. Rev. B **80**, 245120 (2009).
 - ¹³ L.H. Thomas, Proc. Cambridge Phil. Soc. **23**, 542 (1927).
 - ¹⁴ E. Fermi, Atti Accad. Nazl. Lincei **6**, 602 (1927).
 - ¹⁵ R.P. Feynman, N. Metropolis, and E. Teller, Phys. Rev. **75**, 1561 (1949).
 - ¹⁶ F. Perrot, Phys. Rev. A **20**, 586 (1979).
 - ¹⁷ J.W. Dufty and S.B. Trickey, Phys. Rev. B **84**, 125118 (2011).
 - ¹⁸ S. Pittalis, C.R. Proetto, A. Floris, A. Sanna, C. Bersier, K. Burke, and E.K.U. Gross, Phys. Rev. Lett. **107**, 163001 (2011).
 - ¹⁹ N. Troullier and J.L. Martins, Phys. Rev. B **43**, 1993 (1991).
 - ²⁰ N.A.W. Holzwarth, A.R. Tackett, and G.E. Matthews, Comput. Phys. Commun. **135**, 329 (2001).
 - ²¹ P. E. Blöchl, Phys. Rev. B **50**, 17953 (1994).
 - ²² E. Lieb, Rev. Mod. Phys. **48**, 553 (1976).
 - ²³ J. Bartel, M. Brack, and M. Durand, Nucl. Phys. A **445**, 263 (1985).
 - ²⁴ C.H. Hodges, Can. J. Phys. **51**, 1428 (1973).
 - ²⁵ C.F. von Weizsäcker, Z. Phys. **96**, 431 (1935).
 - ²⁶ M. Brack, C. Guet, and H.-B. Hakansson, Phys. Reports **123**, 275 (1985).
 - ²⁷ F. Tran and T.A. Wesolowski, Int. J. Quantum Chem. **89**, 441 (2002).
 - ²⁸ V.V. Karasiev and S.B. Trickey, Comput. Phys. Commun. (2012) (accepted).
 - ²⁹ G.S. Ho, V.L. Lignères, and E.A. Carter, Comput. Phys. Commun. **179**, 839 (2008).
 - ³⁰ L. Hung, C. Huang, I. Shin, G.S. Ho, V.L. Lignères, and E.A. Carter, Comput. Phys. Commun. **181**, 2208 (2010).
 - ³¹ L. Goodwin, R.J. Needs, and V. Heine, J. Phys.: Condens. Matter **2**, 351 (1990).
 - ³² V. Heine, and I.V. Abarenkov, Phil. Mag. **9**, 451 (1964).
 - ³³ J.P. Perdew, and A. Zunger, Phys. Rev. B **23**, 5048 (1981).
 - ³⁴ X. Gonze, B. Amadon, P.-M. Anglade, J.-M. Beuken, F. Bottin, P. Boulanger, F. Bruneval, D. Caliste, R. Caracas, M. Cote, T. Deutsch, L. Genovese, Ph. Ghosez, M. Giantomassi, S. Goedecker, D.R. Hamann, P. Hermet, F. Jollet, G. Jomard, S. Leroux, M. Mancini, S. Mazevet, M.J.T. Oliveira, G. Onida, Y. Pouillon, T. Rangel, G.-M. Rignanese, D. Sangalli, R. Shaltaf, M. Torrent, M.J. Verstraete, G. Zerah, and J.W. Zwanziger, Comput. Phys. Commun. **180**, 2582 (2009); X. Gonze, G.-M. Rignanese, M. Verstraete, J.-M. Beuken, Y. Pouillon, R. Caracas, F. Jollet, M. Torrent, G. Zerah, M. Mikami, Ph. Ghosez, M. Veithen, J.-Y. Raty, V. Olevano, F. Bruneval, L. Reining, R. Godby, G. Onida, D.R. Hamann, and D.C. Allan, Zeit. Kristallogr. **220**, 558 (2005).
 - ³⁵ Paolo Giannozzi, Stefano Baroni, Nicola Bonini, Matteo Calandra, Roberto Car, Carlo Cavazzoni, Davide Ceresoli, Guido L. Chiarotti, Matteo Cococcioni, Ismaila Dabo, Andrea Dal Corso, Stefano de Gironcoli, Stefano Fabris, Guido Fratesi, Ralph Gebauer, Uwe Gerstmann, Christos Gougoussis, Anton Kokalj, Michele Lazzeri, Layla Martin-Samos, Nicola Marzari, Francesco Mauri, Riccardo Mazzarello, Stefano Paolini, Alfredo Pasquarello, Lorenzo Paulatto, Carlo Sbraccia, Sandro Scandolo, Gabriele Sclauzero, Ari P. Seitsonen, Alexander Smogunov, Paolo Umari, and Renata M. Wentzcovitch, J. Phys.: Condens. Matter **21**, 395502 (2009).

³⁶ A.B. Alchagirov, J.P. Perdew, J.C. Boettger, R.C. Albers, and C. Fiolhais, Phys. Rev. B **63**, 224115 (2001).